The Compact Muon Solenoid Experiment

CMS Note

Mailing address: CMS CERN, CH-1211 GENEVA 23, Switzerland
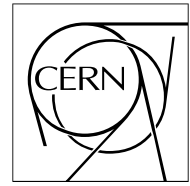
Track Parameter Evaluation and Primary Vertex Finding with the Pixel Detector

S. Cucciarelli, M. Konecki

University of Basel, Switzerland

D. Kotliński

Paul Scherrer Institute, Switzerland

T. Todorov

IN2P3, Strasbourg, France

Abstract

Two algorithms for primary-vertex finding based on charged particle tracks reconstructed with three pixel hits are presented in this note. The evaluation of the track parameters is also described. These algorithms are shown to be suitably fast and efficient for the CMS High Level Trigger.

1 Introduction

Fast and efficient tracking and algorithms for primary-vertex finding are necessary for the High Level Trigger of CMS. Two such algorithms for primary-vertex finding using the Pixel detector information are described in this note.

This note is organised as follows. The Pixel detector is briefly described in Section 2. The determination of the charged particle track parameters, i.e., the transverse momentum and the transverse and longitudinal impact parameters, from the coordinates of three pixel hits, is discussed in Section 3.

Two different approaches for the primary-vertex finding are described and their results are compared in Section 4.

The interface which builds pixel tracks from three pixel hits and both primary-vertex finders have been implemented in the reconstruction software for CMS analysis ORCA [1] (Object-oriented Reconstruction for CMS Analysis).

2 Pixel Detector

The CMS Tracker consists of a Pixel detector and a Silicon Strip detector immersed in a 4 T axial magnetic field provided by a superconducting solenoid. The Pixel detector layout considered in the simulation consists of three barrel layers with two endcap disks on each side. The three barrel layers are located at mean radii 4.4, 7.3 and 10.2 cm and are 53 cm long. The two disks are placed at 34.5 and 46.5 cm from the interaction point. To achieve a similarly good resolution of the vertex position in the transverse and the longitudinal planes, a design with a square pixel shape of dimensions $150 \times 150 \ \mu\mathrm{m}^2$ and thickness $300 \ \mu\mathrm{m}$ is used. The whole Pixel system consists of about 1400 detector modules arranged into half-ladders of four identical modules each in the barrel, and blades with seven different modules each in the endcaps. A more detailed description of the Pixel layout can be found in Ref. [2].

About 16000 readout chips are bump-bonded to the detector modules, for a total of 44 million readout channels. The default noise is set in the simulation at $\sigma = 500$ electrons per pixel and the readout threshold is set at $5 \ \sigma$.

3 Track Parameter Evaluation

Three pixel hits (triplet) are used to form a track, from which the transverse momentum, the longitudinal and transverse impact parameters (IP) are computed. The related studies presented in the following refer to single muon tracks. The hit triplets are made of the first three reconstructed pixel hits associated with this single simulated track.

3.1 Transverse Momentum

A triplet defines a circle in the transverse plane from which the value of the curvature radius R and the transverse momentum $p_T = 3/1000 \cdot \mathrm{B} \cdot R$ (p_T in GeV/c, B in T and R in cm) are extracted. The small lever arm of the Pixel detector, however, allows an accurate estimate to be made only for p_T below $\sim$10 GeV/c.

In Fig. 1, the resolution $\sigma(p_T)/p_T$ is shown as a function of p_T, where $\sigma(p_T)$ is the width of a Gaussian fit of the p_T residual distribution. The relative momentum resolution is well parametrized by $\sigma(p_T)/p_T = 0.055 + 0.17 p_T$ (p_T in GeV/c). Figure 2 shows $\sigma(p_T)/p_T$ for different values of the pseudorapidity η and for a p_T of 1 and 10 GeV/c. For 1 GeV/c, the relative p_T resolution is as good as 7%, but it already amounts to 22% for 10 GeV/c tracks.

3.2 Transverse Impact Parameter

The track transverse impact parameter is defined as the distance of closest approach to the beam axis and is denoted $\mathrm{IP}_{r\phi}$. The transverse impact parameter is determined from the centre coordinates $(x_\mathrm{C}, y_\mathrm{C})$ and the radius R of the unique circle that passes through the three pixel hits. The unsigned distance of closest approach of the circle to the beam axis is used as an estimate of $\mathrm{IP}_{r\Phi}$:

$$\mathrm{IP}_{r\Phi} = |\sqrt{x_\mathrm{C}^2 + y_\mathrm{C}^2} - R|.$$
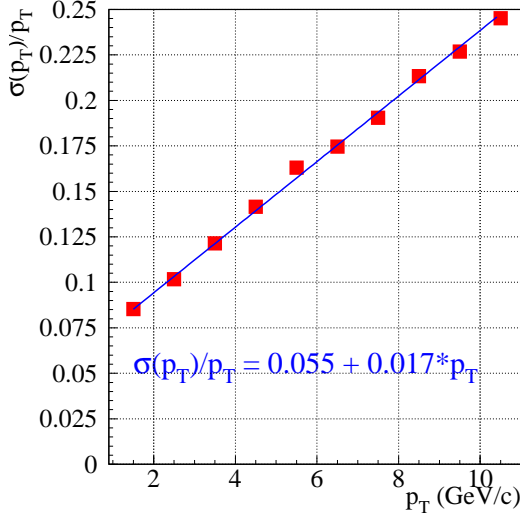
Figure 1: Linear behaviour of $\sigma(p_T)/p_T$ as a function of p_T, for single muon tracks.
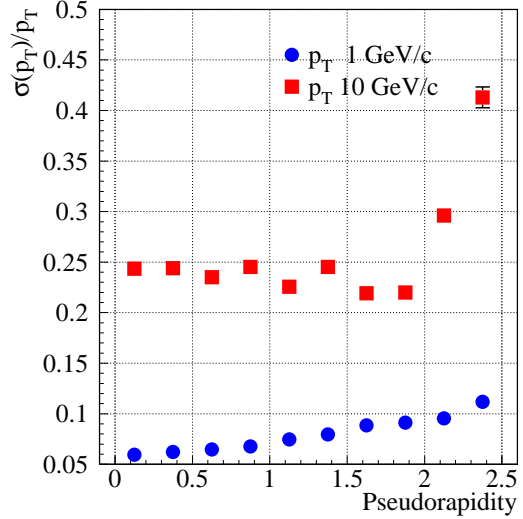
Figure 2: The p_T resolution as a function of the pseudorapidity for single muon tracks with p_T of 1 and $10\,\text{GeV}/c$.

For large transverse momentum, this expression is a difference between two large terms, which may lead to numerical inaccuracies. To alleviate this potential problem, the circle through the pixel hits may always be approximated by a parabola [3], the equation of which is expressed with the reduced coordinates

$$u = \frac{x}{x^2 + y^2}, \quad v = \frac{y}{x^2 + y^2},$$

as $v = p_1 + p_2 u + p_3 u^2$, with

$$p_1 = \frac{1}{y_C}, \quad p_2 = -\frac{x_C}{y_C}, \quad p_3 = -\left(\frac{R}{y_C}\right)^3 \text{IP}_{r\Phi}.$$

The transverse impact parameter resolution is shown in Fig. 3 as a function of p_T and for the two pseudorapidity regions $|\eta| < 1.7$ and $|\eta| > 1.7$. Above $6\,\text{GeV}/c$, the transverse impact parameter resolution is around $80\,\mu$m. When the hits from the Silicon Tracker detector are used as well, this resolution is improved to $20\,\mu$m.

3.3 Longitudinal Impact Parameter

To estimate the longitudinal impact parameter, z_{IP}, both a linear approximation and the complete helix parametrization were implemented and tested for the HLT.

In the first case, the three pixel hits are projected onto the (r, z) plane, and their coordinates are fit in this plane to a straight line. The longitudinal impact parameter is defined as the point of intercept between this line and the z axis.

A higher accuracy can be reached, however, with the full helix parametrization. The three pixel hits are now projected onto the (ψ, z) plane, where ψ is the azimuthal angle difference between the hit and the point of closest approach around the circle defined by the three hits (Section 3.2). In this plane, the helix projection is expected to be exactly a straight line, up to the uncertainties due to the hit position measurement and the multiple scattering in the detector material. The longitudinal impact parameter is defined as the point of intercept between the line joining the first two pixel hits $(\psi_{1,2}, z_{1,2})$ and the z axis :

$$z_{\text{IP}} = z_1 - \frac{\psi_1}{\psi_1 - \psi_2}(z_1 - z_2). \tag{1}$$

3
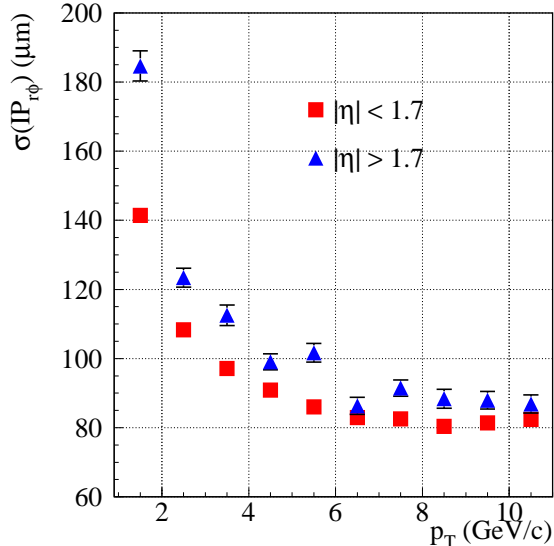
Figure 3: Transverse impact parameter resolution as a function of p_T, for two different pseudorapidity regions.

The longitudinal IP resolution, $\sigma_{z_{IP}}$, is shown in Figs. 4 and 5 as a function of pseudorapidity η for three different values of p_T, both in the linear approximation and with the helix parametrization. The helix parametrization is always better than the linear approximation by 40 to 50%.

The longitudinal impact parameter is of prime importance in the determination of the primary-vertex z position (Section 4). Its resolution is therefore a crucial input. For this reason, the $\sigma_{z_{IP}}$ dependence on p_T was parametrized in three pseudorapity ranges, $0 < |\eta| < 0.8$, $0.8 < |\eta| < 1.6$ and $|\eta| > 1.6$. As a cross check, Fig. 6 shows the distribution of $(z_{IP}^{rec} - z_{IP}^{sim})/\sigma_{z_{IP}}$ for single muon tracks with a p_T from 1 to 10 GeV/c in the Pixel detector acceptance. The longitudinal IP resolution is improved by a factor of two by the use of the full Tracker information.

The quality of the track entering the primary-vertex determination needs also to be quantified. The χ^2 of the linear fit in the (r, z) plane is retained for this purpose. In this χ^2, the uncertainty on the hit positions is assumed to be the quadratic sum of the detector resolution [4] and the expected multiple scattering contribution.

4 Primary Vertex Finding

The primary-vertex finding based on pixel hits provides to the trigger the first primary-vertex position measurement. This measurement is subsequently used for track seeding and in most High-Level Trigger (HLT) analyses. It must therefore be fast and precise enough. For this reason primary-vertex finding is reduced here to a one-dimensional search along the z axis.

The relevant sets of three hits are collected by the triplet finding algorithm described in Ref. [5]. All the results presented in the following refer to hit triplets found in the full Pixel detector acceptance. (It is also possible to restrict the triplet finding to selected regions of the Tracker detector, so as to render the vertex finding faster and more flexible.) The detailed performance study reported here refers to the vertex finding in q$\bar{q}$ events with 17.3 pileup events per beam crossing, as will be the case at high luminosity in the LHC. Many different simulated event samples, at high and low luminosity, were also studied, and the corresponding performance figures are summarized here as well. The minimum bias and the underlying events were generated with PYTHIA [6] as described in Ref. [7]. Because the performance of primary-vertex finding depends strongly on the charged-particle multiplicity and p_T spectrum, the efficiencies in this note have to be considered with caution. Different models could indeed lead to substantially different figures.

Two vertex-finding algorithms were tested and implemented in the HLT. The Histogramming Method progressively merges tracks close enough to each other in z_{IP}, to form primary-vertex candidates, denoted 'PV Clusters' in the following. The Divisive Method looks for large z_{IP} intervals without tracks to divide the z axis in several regions. In both methods, an average primary-vertex position is computed from all tracks in each of the PV clusters, and
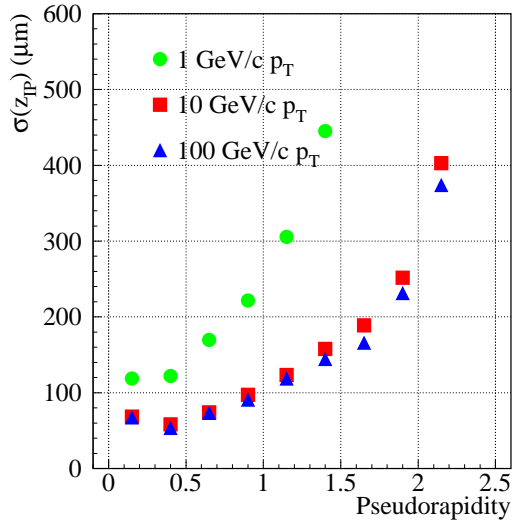
Figure 4: Resolution of the longitudinal impact point from the linear approximation, as a function of η and for for p_T values 1, 10 and 100 GeV/c.
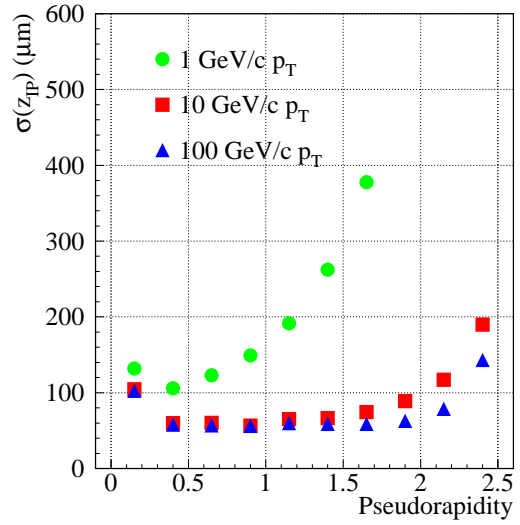
Figure 5: Resolution of the longitudinal impact point from the helix parametrization, as a function of η and for for p_T values 1, 10 and 100 GeV/c.
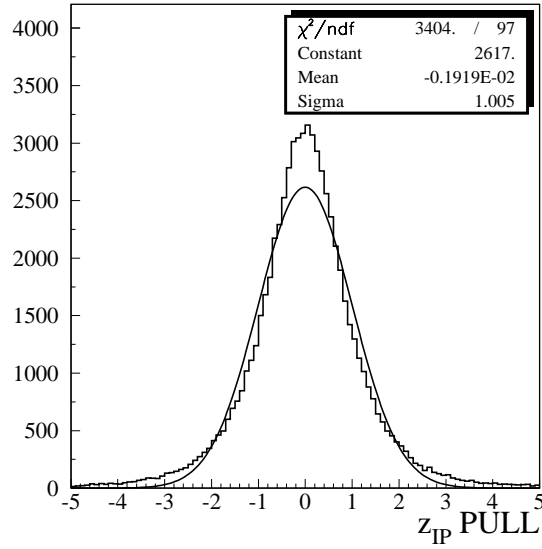
Figure 6: Pull distribution of the longitudinal IP for single muon tracks with p_T from 1 to 10 GeV/c in the full Pixel detector acceptance.

tracks not compatible with that average position are discarded. The procedure iterates and stops when all tracks are found to be compatible with the corresponding primary vertex positions.

Among the primary-vertex candidates, the *closest* primary vertex is defined as that closest in z to the simulated signal PV and the *tagged* primary vertex as that chosen as the signal primary vertex of the event.

For a given event, the primary vertex (tagged or closest) is *found* if it is reconstructed inside a window of 500 μm around the true PV position. The PV-finding efficiency is the fraction of events with a *found* (tagged or closest) primary vertex. The closest PV-finding efficiency evaluates the ability of the algorithm in finding a PV candidate. The tagged PV-finding efficiency evaluates the ability of the algorithm in identifying the signal PV of the event.

Only pixel tracks reconstructed with p_T in excess of 1 GeV/c, a transverse IP smaller than 1 mm and χ^2 value smaller than 100, are considered in the following.

A *good* track is a pixel track associated to a simulated track coming from the signal primary vertex. The association of a pixel track to a simulated track requires each of the three reconstructed hits to be associated to a hit of the simulated track. All other tracks are called *bad* tracks. Bad tracks are either ghost tracks or tracks coming from pileup events. The track-to-vertex association efficiency and the ghost-to-vertex association rate are defined as follows:

$$\text{Track Association Efficiency} = \frac{N_{\text{PVCluster}}^{\text{TkGood}}}{N_{\text{Event}}^{\text{TkGood}}}, \tag{2}$$

$$\text{Track Association Ghost Rate} = \frac{N_{\text{PVCluster}}^{\text{TkBad}}}{N_{\text{PVCluster}}^{\text{Tk}}}, \tag{3}$$

where $N_{\text{PVCluster}}^{\text{TkGood}}$ is the number of good tracks in the PV cluster, $N_{\text{Event}}^{\text{TkGood}}$ the total number of good tracks in the event, $N_{\text{PVCluster}}^{\text{TkBad}}$ the number of bad tracks in the PV cluster and $N_{\text{PVCluster}}^{\text{Tk}}$ is the total number of tracks in the PV cluster.

4.1 Histogramming Method

The tracks are first merged in the 5000 bins of a histogram of their longitudinal IP, z_{IP}, in a ± 15 cm window around the nominal interaction point. An example of such an histogram is shown in Fig. 7 for a q$\bar{\text{q}}$ event at high luminosity. Only the non-empty bins are kept, and their position is computed as the track z_{IP} simple average. These non-empty bins are then scanned along z. A PV cluster is defined as a continuous set of consecutive bins separated by less than a certain threshold Δz. The z position of the PV cluster, z_{PV}, is determined by averaging the z_{IP} of all tracks associated to this cluster.
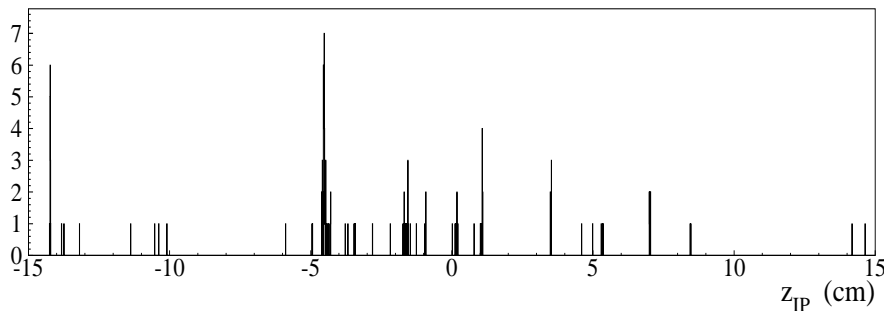
Figure 7: The distribution of the longitudinal IP for a high luminosity q$\bar{\text{q}}$ event with $E_t = 100$ GeV.

A cleaning procedure is applied to each PV cluster, rejecting the tracks distant from the PV-cluster position by more than z_{offset} standard deviations away from the cluster, i.e., such that

$$|z_{\text{IP}} - z_{\text{PV}}| < z_{\text{offset}} \cdot \sigma_{z_{\text{IP}}},$$

where $\sigma_{z_{\text{IP}}}$ is parametrized as explained in Section 3.3. The z position of the PV clusters is recomputed with the remaining tracks, and the procedure iterates until each remaining track is declared compatible with its associated PV cluster according to the above criterion. The performance of the algorithm depends on the parameters Δz and

z_{offset}. It was tested with these parameters varying in the ranges from 0.1 to 2.6 mm and from one to seven standard deviations, respectively.

For each PV cluster, the quantity $S = \sum p_T'^2$ is computed, where the sum runs over all the associated tracks and

$$p_T' = \begin{cases} 0 & \text{if } p_T < 2.5 \text{ GeV}/c, \\ p_T & \text{if } 2.5 \text{ GeV}/c < p_T < 10 \text{ GeV}/c, \\ 10 & \text{if } p_T > 10 \text{ GeV}/c. \end{cases} \quad (4)$$

The PV cluster with the largest S value is called the tagged PV, by definition. In the S evaluation, the tracks with a very small p_T likely originating from pileup events, are not considered. A threshold is set at high momentum not to overweight vertices with very few high-momentum tracks, determined with a poor resolution.

The performance of the algorithm is found to be only mildly dependent on the choice of z_{offset} between one and three standard deviations. The default value for z_{offset} was therefore set to 1.0 in the following. Figure 8 shows the PV-finding efficiency for different values of Δz, for both the closest and tagged primary vertex. The best performance of the algorithm is reached for small values of the merging parameter due to the pollution of pileup events at high luminosity. Indeed, for large Δz values, many bins are merged together and the PV cluster is associated to many bad tracks. The averaged z_{PV} value is therefore far from the true position, and the PV is subsequently not *found*.
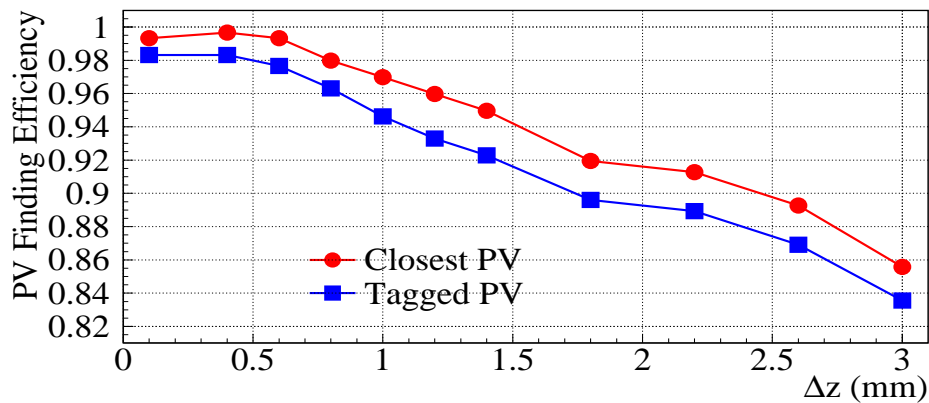
Figure 8: The PV-finding efficiency of the histogramming method. Efficiencies for the closest (circle) and tagged (square) primary vertex of the event are shown as a function of the merging parameter Δz, for high luminosity q$\bar{\text{q}}$ events with $E_t = 100$ GeV.

The track association efficiency and ghost rate as a function of Δz are shown in Fig. 9. Efficiencies close to 100% are reached for $\Delta z \leq 0.6$ mm, for which the track ghost rate is around 10%.

Figure 10 displays the resolution of the z-position of the primary vertex as a function of the merging parameter. The resolution is dtermined from a Gaussian fit to the residual distributions. For $\Delta z = 0.6$ mm, the primary vertex is found with a resolution of about 50 μm.

The algorithm was applied with these tuned parameters ($z_{\text{offset}}=1.$, $\Delta z = 0.6$ mm) to other event samples. The corresponding PV-finding efficiencies are listed in Table 1. For most event samples the primary vertex is recovered with an efficiency close to 100%. Efficiencies of primary-vertex finding are significantly below 100% for events like h $\rightarrow \gamma\gamma$, where the small average number of charged particle tracks does not allow the signal PV to be always distinguished from pileup primary vertices. Other methods specific to h $\rightarrow \gamma\gamma$ are under investigation.

4.2 Divisive Method

The same set of tracks as for the histogramming method is used in the divisive method. In this method, the tracks are ordered according to increasing z_{IP}. The ordered list is scanned to form a PV cluster until a pair of consecutive tracks separated by more than a certain threshold z_{sep} is found, at which point another PV cluster is built. The position of each of these PV clusters is determined iteratively as explained in Section 4.1, according to the parameter z_{offset}.
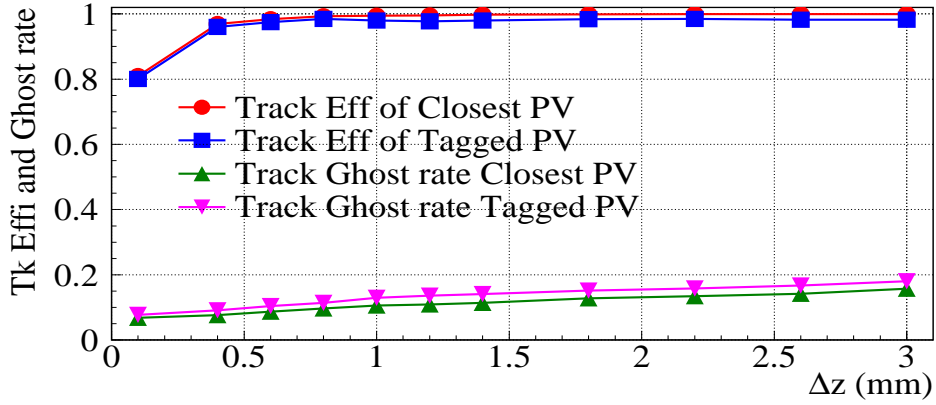
Figure 9: Track association efficiency and ghost rate of the histogramming method as a function the merging parameter Δz for high luminosity q$\bar{\text{q}}$ events with $E_t = 100\,\text{GeV}$.
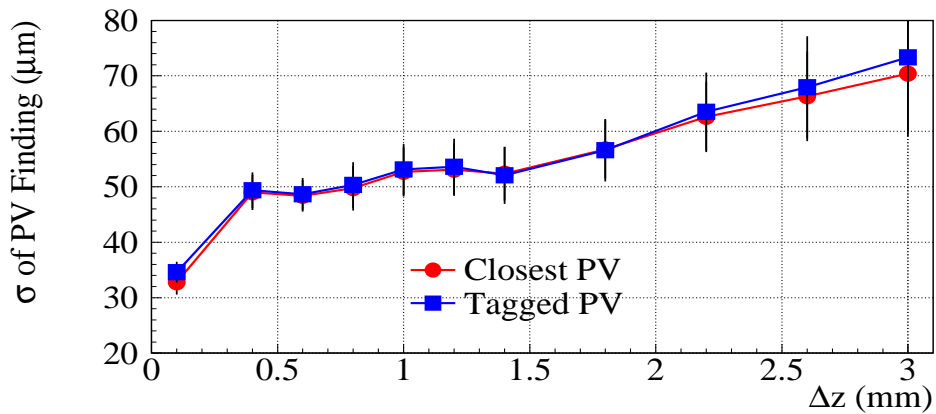
Figure 10: Resolution of the PV z-position obtained with the histogramming method, as a function of the Δz parameter and for high luminosity q$\bar{\text{q}}$ events with $E_t = 100\,\text{GeV}$.

Table 1: Tagged and closest PV-finding efficiencies of the histogramming method, for different samples of events at high and low luminosity.

Event Type	High Lumi		Low Lumi	
	Closest PV Eff	Tagged PV Eff	Closest PV Eff	Tagged PV Eff
$q\bar{q}\ E_T^{\mathrm{Jet}} = 100$ GeV	0.99	0.98	1.00	0.99
$b\bar{b}\ E_T^{\mathrm{Jet}} = 100$ GeV	0.98	0.95	0.99	0.99
QCD $\hat{p}_T = 120 \div 170$ GeV/c	0.98	0.97	1.00	0.99
QCD $\hat{p}_T = 50 \div 80$ GeV/c	0.96	0.80	0.97	0.80
$B_s \to \mu\mu$	0.90	0.52	0.92	0.80
$h \to ZZ\ m_h = 130$ GeV/c^2	0.97	0.93	0.98	0.98
$h \to WW\ m_h = 140$ GeV/c^2	0.93	0.81	0.96	0.94
$h \to \gamma\gamma\ m_h = 115$ GeV/c^2	0.91	0.55	0.92	0.78

The whole recipe is applied again to the tracks discarded in the PV-cluster-position determination procedure, for each PV cluster. New PV clusters are built iteratively, until the number of remaining tracks is smaller than $N_{\mathrm{Tk}}^{\mathrm{min}}$. (Here, the choice $N_{\mathrm{Tk}}^{\mathrm{min}} = 2$ is made.) The tagged PV cluster is defined as in Section 4.2, i.e., according to the largest value of S.

The performance of divisive PV-finding in a a high luminosity environment is sensitive to both the z_{sep} and the z_{offset} parameters. Figure 11 shows the closest and tagged PV-finding efficiencies as a function of the z_{sep} parameter with z_{offset} set to five standard deviations, at high luminosity. Values of the PV-finding efficiency above 95% are reached for small values of the separation parameter, below 1 mm. For larger values of z_{sep}, the original PV clusters contain many (bad) tracks. The z_{PV} value is therefore far from from the true position, many good tracks are discarded and the PV is subsequently not *found*.
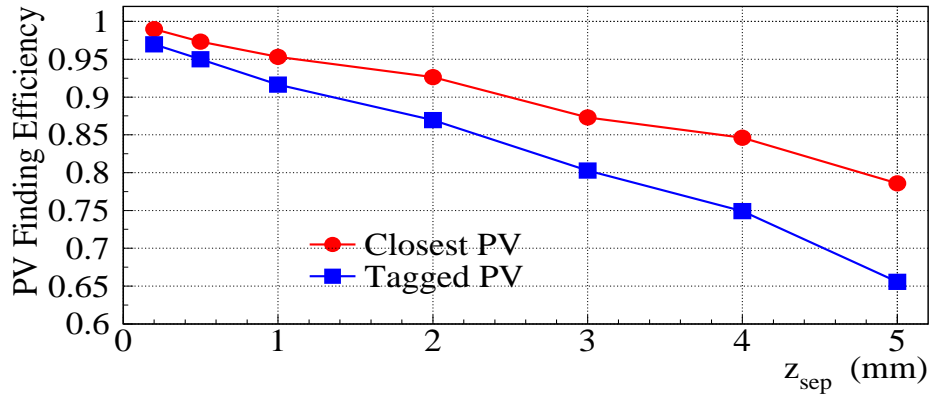
Figure 11: The PV-finding efficiency of the divisive method. Efficiencies for the closest (circle) and tagged (square) primary vertex of the event are shown as a function of the parameter z_{sep}, for high luminosity $q\bar{q}$ events with $E_T = 100$ GeV. The z_{offset} value corresponds to five standard deviations.

The track-to-PV association efficiency and the ghost rate are shown in Fig. 12 as a function of z_{sep}. An efficiency above 90% and a ghost rate smaller than 10% are achieved for small values of z_{sep}. For values of z_{sep} smaller than 0.5 mm, the track-to-PV association efficiency starts to decrease. A value of z_{sep} of 0.5 mm allows the PV-finding efficiency to be larger than 95% keeping the track-to-PV association efficiency above 90%.

In order to have high values of the PV-finding efficiency at low luminosity, the value of z_{sep} has to be even smaller than 100 μm. The closest and tagged PV-finding efficiencies for $q\bar{q}$ at low luminosity are shown in Fig. 13, for values of the z_{sep} parameter below 200 μm. To obtain a PV-finding efficiency larger than 95% while keeping a high track-to-PV association efficiency, z_{sep} should be set to 50 μm.
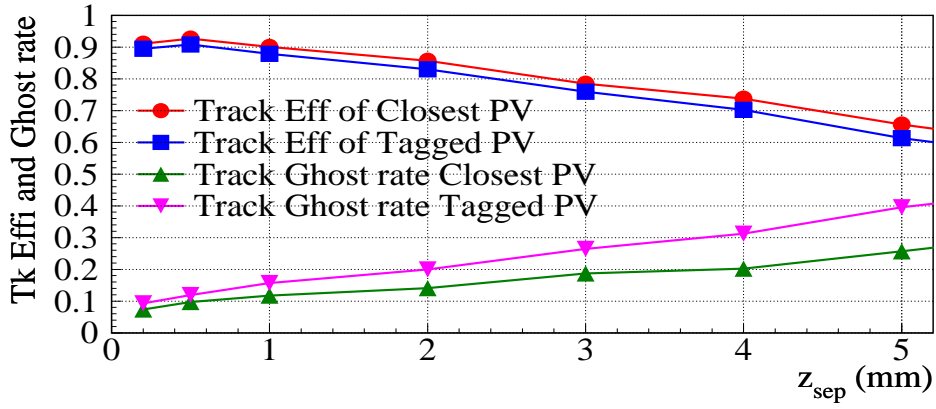
Figure 12: Track association efficiency and ghost rate of the divisive method as a function the z_{sep} parameter for high luminosity $q\bar{q}$ events with $E_T =100\,\text{GeV}$. The z_{offset} value corresponds to five standard deviations.
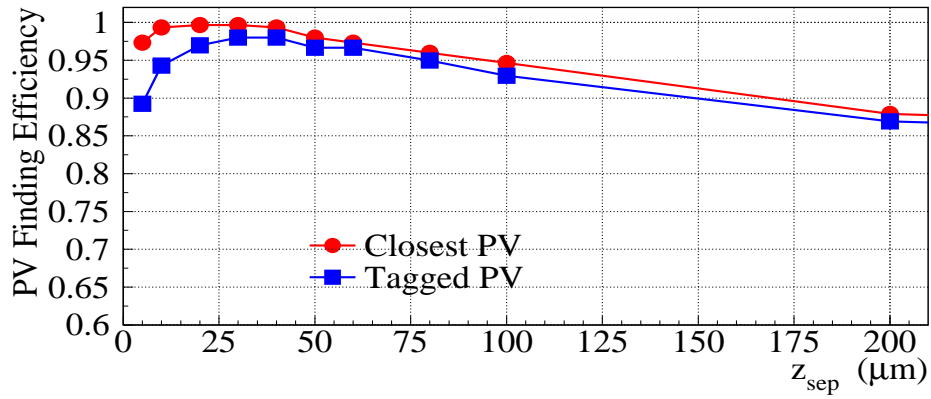
Figure 13: The PV-finding efficiency of the divisive method. Efficiencies for the closest (circle) and tagged (square) primary vertex of the event are shown as a function of the parameter z_{sep}, for low luminosity $q\bar{q}$ events with $E_T =100\,\text{GeV}$. The z_{offset} value corresponds to five standard deviations.

The PV-finding efficiency is shown in Fig.14 as a function of z_{offset}. Large value of z_{offset} (in excess of 4.0) are required to bring the tagged PV efficiency close to 100%. This effect is reflected also in the track association efficiency as is shown in Fig. 15. Below three standard deviations, the track association efficiency is small and the position of the primary vertex candidate is far from the true one.
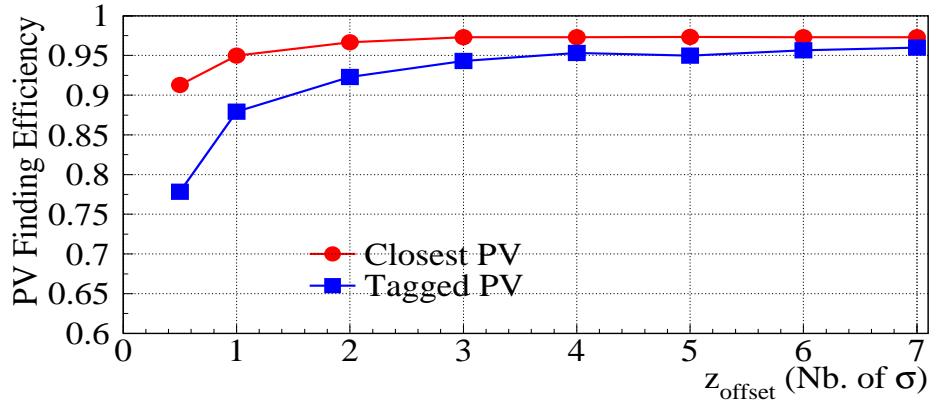
Figure 14: The PV-finding efficiency of the divisive method. Efficiencies with respect to the closest (circle) and tagged (square) primary vertex of the event are shown as a function of the parameter z_{offset}, for high luminosity $q\bar{q}$ events with $E_T = 100\,\text{GeV}$. The z_{sep} value is set to 0.5 mm.
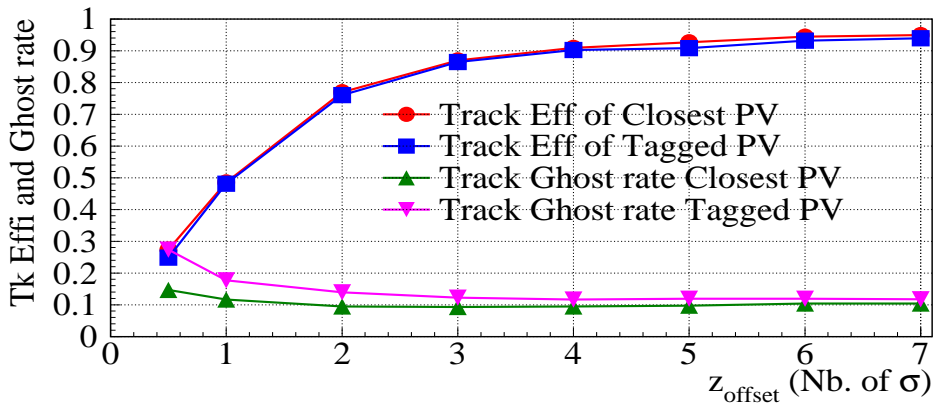
Figure 15: Track association efficiency and ghost rate of the divisive method as a function of the z_{offset} parameter, for high luminosity $q\bar{q}$ events with $E_T = 100\,\text{GeV}$. The z_{sep} value is set to 0.5 cm.

Figure 16 shows the resolution of the PV z-position measurement as a function of the z_{sep} parameter as obtained from a Gaussian fit of the residual distributions. For $z_{\text{sep}} = 0.5\,\text{mm}$ and $z_{\text{offset}} = 5$., the primary vertex is found with a resolution of about 50 μm.

This algorithm was applied with these tuned parameters ($z_{\text{offset}} = 5.$, $z_{\text{sep}} = 0.5\,\text{mm}$ and 50 μm for high and low luminosity events) to other event samples. Table 2 presents the efficiencies of the primary vertex finding at high and low luminosity. In general, the results obtained with the divisive algorithm are very similar to those obtained with the histogramming method.

4.3 Timing

The average time per event needed for the track parameter evaluation is about 7 ms per event. The average time for the primary-vertex finding is 0.7 ms per event, for both the histogramming and divisive methods. The time was measured on a 2.8 GHz PentiumIV and for $q\bar{q}$ events with $E_T^{\text{Jet}} = 100$ GeV at high luminosity. The time quoted does not include the contributions from the hit reconstruction and the triplet finding.

11
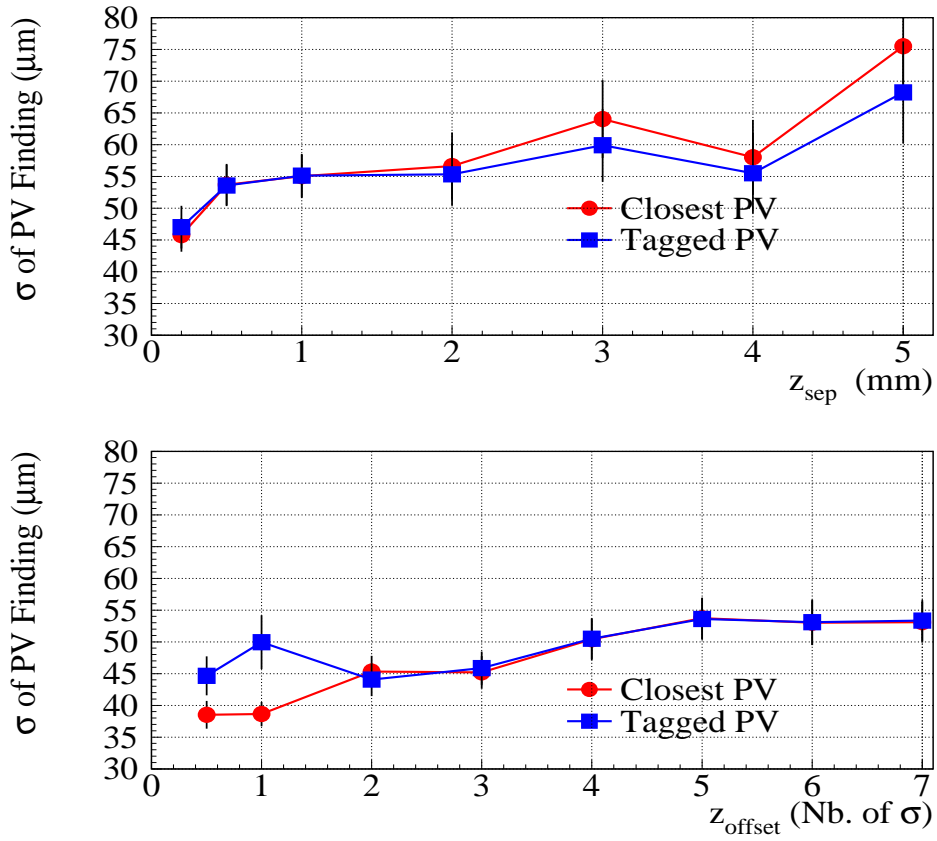
Figure 16: Resolution of the PV z-position obtained with the divisive method, (top) as a function of z_{sep} with z_{offset} set to five standard deviations and (bottom) as a function of z_{offset} with z_{sep} set to 0.5 mm, for high luminosity q$\bar{\mathrm{q}}$ events with $E_T =100\,\mathrm{GeV}$.

Table 2: Tagged and closest PV-finding efficiencies of the divisive method, for different samples of events at high and low luminosity.

Event Type	High Lumi		Low Lumi	
	Closest PV Eff	Tagged PV Eff	Closest PV Eff	Tagged PV Eff
$q\bar{q}$ $E_T^{\mathrm{Jet}} = 100$ GeV	0.99	0.97	0.98	0.97
$b\bar{b}$ $E_T^{\mathrm{Jet}} = 100$ GeV	0.99	0.90	1.00	0.96
QCD $\hat{p}_T = 120 \div 170$ GeV/c	1.00	0.97	1.00	0.96
QCD $\hat{p}_T = 50 \div 80$ GeV/c	0.97	0.80	0.98	0.92
$B_s \to \mu\mu$	0.97	0.50	0.96	0.71
$h \to ZZ$ $m_h = 130$ GeV/c^2	0.98	0.95	0.99	0.98
$h \to WW$ $m_h = 140$ GeV/c^2	0.99	0.85	0.97	0.94
$h \to \gamma\gamma$ $m_h = 115$ GeV/c^2	0.96	0.52	0.94	0.75

5   Conclusions

The parameter evaluation for tracks reconstructed with three pixel hits and two different algorithms for primary-vertex finding with these pixel tracks as input have been presented. Efficiencies of primary-vertex reconstruction in excess of 90% are obtained for large multiplicity events, with a z-position resolution of the order of 50 microns, for both methods, at low and high luminosities.

References

[1] See http://cmsdoc.cern.ch/orca.

[2] The CMS Collaboration, *"CMS Tracker Technical Design Report"*, **CERN/LHCC 1998/06**.

[3] M. Hansroul et al., *"Fast Circle Fit with the Conformal Mapping Method"*, Nucl. Instrum. and Methods; **A270** (1998), 498-501.

[4] S.Cucciarelli, D. Kotlinski and T. Todorov, *"Position Determination of Pixel Hits"*, **CMS Note2002/049**.

[5] S. Cucciarelli, M. Konecki, D. Kotlinski and T. Todorov, *"Track Finding Using the Pixel Detector"* CMS Note in preparation.

[6] T. Sjostrand et al., *"High Energy Physics Event Generation with PYTHIA 6.1"*, **HEP-PH/0010017**.

[7] The CMS Collaboration, *"Data Acquisition and High Level Trigger Technical Design Report"*, **CERN/LHCC 2002/26**.